View Article Online / Journal Homepage / Table of Contents for this issue

J-aggregate formation in bis-(4-carboxyphenyl)porphyrins in water : pH and counterion dependence†

Vanda Vaz Serra,[a] Suzana M. Andrade,[b] Maria G. P. M. S. Neves,*[a] José A. S. Cavaleiro[a] and Sílvia M. B. Costa*[b]

Received (in Gainesville, FL, USA) 16th March 2010, Accepted 9th June 2010
DOI: 10.1039/c0nj00201a

Published on 26 August 2010 on http://pubs.rsc.org | doi:10.1039/C0NJ00201A
Downloaded by University of Belgrade on 02 January 2013

The self aggregation behaviour of *meso*-tetraarylporphyrins containing two carboxyphenyl units in adjacent and opposite positions, respectively, 5,10-bis(4-carboxyphenyl)-15,20-diphenylporphyrin (**DiCPP-adj**) and 5,15-bis(4-carboxyphenyl)-10,20-diphenylporphyrin (**DiCPP-opp**), was investigated at different pH values. Ordered porphyrin architectures are obtained at pH = 0.8 and pH = 12 for both compounds studied, through an easy self assembly approach. The type of architecture and the extent of aggregation are related with the relative positions of the 4-carboxyphenyl groups attached to the porphyrin core and with the counterions present. The aggregates obtained exhibit spontaneous chirality, resonance light scattering, short fluorescence lifetimes and low fluorescence quantum yields. The data gives evidence that at pH = 0.8 with NO_3^- the preferred aggregation is more favoured for **DiCPP-adj** than for **DiCPP-opp**, whereas at pH = 12 the aggregate of **DiCPP-opp** is induced by Na^+ and Li^+ cations and stabilized by hydrophobic interactions. Deposition of aqueous solutions at key pHs on glass surfaces enables the detection of circular and ring aggregates viewed by fluorescence lifetime imaging microscopy (FLIM) with dimensions of a few micrometres.

Introduction

The ability of porphyrins and metalloporphyrins to aggregate in special organized geometries by non-covalent approaches has been explored in the preparation of new supramolecular systems based on porphyrinic arrays.[1,2] The self-assembly strategy offers a significant number of advantages when compared to the covalent bonding based synthesis of multi-porphyrinic arrays; the former approaches are usually easier, efficient and do not need time consuming and expensive purification steps.[3,4] However, functionalization with adequate coordinative groups correctly distributed and oriented in the porphyrinic frame is essential for a good design of supramolecular self-assembled systems. Naturally occurring and synthetic water soluble porphyrins like protoporphyin-IX and *meso*-tetrakis(*p*-sulfonatophenyl) porphyrin (TSPP) can form organized geometrical arrangements usually classified as J-aggregates (side-by-side) or H-aggregates (face-to-face).[5] J-aggregates are the most interesting ones and can exhibit interesting nonlinear optical and optoelectronic properties. The formation of J-aggregates has also been reported for water insoluble porphyrins like *meso*-tetra(*p*-hydroxyphenyl)porphyrin (THPP) in non ionic Triton-X and in the presence of trihaloacetic acids.[6]

Amphiphilic molecules such as *meso*-carboxyphenylporphyrins (large hydrophobic porphyrinic frame and easily ionisable carboxylic groups) are expected to form supramolecular assemblies also. Recently, the aggregation pattern of *meso*-tetrakis(*p*-carboxyphenyl)porphyrin (TCPP) was investigated in the presence of polyvinylalcohol (PVA) at a pH below 1 using different acids (trifluoroacetic acid, HNO_3 and HCl).[7,8] Another interesting study reported the formation of J- and H-aggregates of TCPP in micellar systems using different surfactants.[9]

Porphyrins with ionisable substituents, like *meso*-carboxyphenyl porphyrins, can assume both cationic and anionic forms in homogeneous acid or basic solutions. Dicationic porphyrins can be easily formed at acid pH since the protonation of the inner nitrogens occurs at a pH of around 5. At higher pH the inner nitrogen atoms are not protonated and the carboxyphenyl substituents are present in the carboxylate form (pK_a of the carboxylic groups is approximately 5–7)[10] affording anionic porphyrins.

Spectral changes in the UV-vis light region are related with the aggregation profile of this kind of molecule. According to Kasha's exciton theory, bathochromic (red) shifts are expected for the absorption bands of J-aggregates when compared with the typical absorption bands of corresponding monomers and hypsochromic (blue) shifts are reported for H-aggregates.[11]

Our goal is to find the relationship between the substitution position, global charges of aggregate structures and the shape of micrometre/nanometric-sized domains upon variation of the pH aqueous solution. Towards this aim, the self-aggregation patterns of two substituted carboxyphenyl porphyrins: 5,15-bis(4-carboxyphenyl)-10,20-diphenylporphyrin (**DiCPP-opp**)

[a] *Departamento de Química, Universidade de Aveiro, Campus Universitário de Santiago, 3810-193 Aveiro, Portugal. E-mail: gneves@ua.pt; Fax: +351 234 370084; Tel: +351 234 370710*
[b] *Centro de Química Estrutural, Complexo I; Instituto Superior Técnico, Av. Rovisco Pais, 1049-001 Lisbon, Portugal. E-mail: sbcosta@mail.ist.utl.pt; Fax: +351 21 8464455; Tel: +351 21 8419000*

† Electronic supplementary information (ESI) available: Additional spectroscopic and kinetic experimental data. See DOI: 10.1039/c0nj00201a

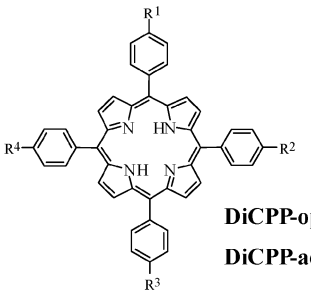

DiCPP-opp: $R^1 = R^3 = H$; $R^2 = R^4 = CO_2H$

DiCPP-adj: $R^1 = R^2 = H$; $R^3 = R^4 = CO_2H$

Scheme 1 Molecular structure of porphyrins.

Published on 26 August 2010 on http://pubs.rsc.org | doi:10.1039/C0NJ00201A
Downloaded by University of Belgrade on 02 January 2013

and 5,10-bis(4-carboxyphenyl)-15,20-diphenylporphyrin (**DiCPP-adj**) (Scheme 1) were investigated. These porphyrins are isomers with two carboxyphenyl units in opposite and adjacent positions, respectively. The self-aggregation properties in aqueous solution were evaluated by absorption, steady state and transient state fluorescence spectroscopy, at different pH values and in the absence of a stabilizer. The formation and the extension of the aggregates were also investigated by resonance light scattering (RLS) and circular dichroism (CD). Fluorescence lifetime imaging microscopy (FLIM) was used to understand better the size and shape of porphyrin aggregates. In this paper, we would like to show that the overall data gave evidence of the formation of organized pH induced structures in aqueous solutions without the need of a stabilizer. These are affected by the relative positions of the *meso*-carboxyphenyl substituents and counter-ions present, suggesting a different self-assembly organization for **DiCPP-opp** and **DiCPP-adj**.

Results

The electronic absorption spectra of the disubstituted porphyrins **DiCPP-opp** and **DiCPP-adj** in DMSO showed the expected typical features of monomeric species (see Table 1). Acidic solutions of DMSO/HCl and water/HCl pH 0.8 showed dicationic monomeric species (see Table 1). It is well known that at different pH values significant structural modifications occur that markedly affect the characteristic UV-vis spectra of monomeric porphyrins.[12]

The electronic spectra of each porphyrin collected at pH range 2 to 5 show broad bands suggesting the overlapping spectra of different species, namely of neutral and dicationic monomers and of non specific aggregates. The low solubility of these porphyrins in water at this pH range can also contribute to the broad band profile detected.

A completely different behaviour is observed when aggregates are promoted in aqueous solutions of HNO_3 at pH 0.8 or in aqueous solutions above pH 7. The derivatives' corresponding absorbance spectra show significant changes at these key pH values. In order to simplify the discussion of results obtained, the absorption and steady-state fluorescence spectroscopy data will be presented first for each derivative, followed by the ones obtained by RLS and CD techniques.

Aggregation studies by absorption and steady state fluorescence spectroscopy

DiCPP-opp. The optical spectrum of **DiCPP-opp**, with the two carboxylphenyl units in opposite positions, shows at pH 12 important differences when compared with the ones obtained for the same porphyrin in the monomeric form.

At pH 12, the Soret band of the neutral monomeric species (centred at 419.5 nm in DMSO, see Table 1) can only be detected as a shoulder. Instead, two new bands appear: a broad one, blue shifted and centred at 365 nm and a major narrow one red shifted and centred at 446 nm (Fig. 1A). The Q bands' wavelength maxima are also red shifted. The band at 446 nm suggests the formation of J-type aggregates and this possibility is supported by steady-state fluorescence spectroscopy, RLS and CD data which will be discussed later. The significant disappearance of the characteristic absorption band of the monomeric species seems to indicate a large tendency for porphyrin **DiCPP-opp** to form aggregates under these experimental conditions. These species are also formed at neutral pH values. However, a slight increase of the intensities of the Soret band and of the second Q band with increasing pH values from 7 to 12 confirm that the formation of the new aggregate is favoured at higher pH values.

The excitation spectra obtained from the fluorescence at different wavelengths present a similar Soret band maximum (~414 nm) although the absorption spectra do not match (Fig. 1A). These aspects reinforce the hypothesis of aggregation, since aggregates have a considerably lower quantum yield comparative to that of monomers and thus, the fluorescence detected arises essentially from the monomers.

Table 1 Peak position for the UV-Vis absorption and fluorescence emission (nm) spectra of porphyrins (5 μM) in DMSO, DMSO/HCl and aqueous solution at different pH

Porphyrin	Medium	Absorption		Fluorescence
		Soret	Q-bands	Q-bands
DiCPP-opp	DMSO	419.5	516, 550, 591, 647.5	650, 716.5
	DMSO/HCl	452	615, 665	—
	pH = 0.8[a]	436.5, 496	723.5	680[b] (680, 755)[c]
	pH = 12	446	532, 569, 610, 663	650, 712.5 (665.5, 736)[d]
DiCPP-adj	DMSO	419	516, 550, 591, 647	651, 717
	DMSO/HCl	452	615, 666	—
	pH = 0.8[a]	434, 494	713.5	678 (750)[c]
	pH = 0.8[e]	434	598, 649	680[b]
	pH = 12	415.5 (400, 445)[f]	518, 554, 596, 649.5	(653, 720)[g]

[a] With HNO_3. [b] λ_{exc} = 436 nm. [c] λ_{exc} = 496 nm. [d] λ_{exc} = 446 nm. [e] With HCl. [f] Shoulder. [g] λ_{exc} independent.

 This journal is © The Royal Society of Chemistry and the Centre National de la Recherche Scientifique 2010

Published on 26 August 2010 on http://pubs.rsc.org | doi:10.1039/C0NJ00201A
Downloaded by University of Belgrade on 02 January 2013

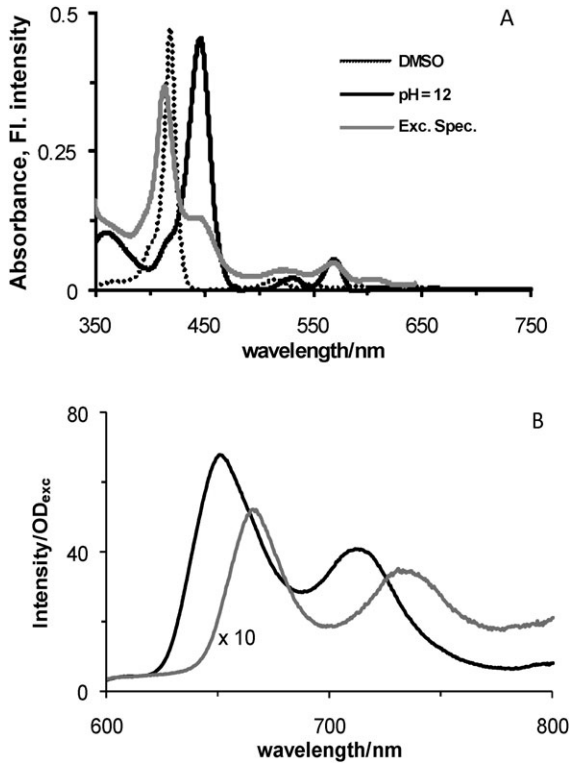

Fig. 1 (A) UV-Vis spectra of **DiCPP-opp** (5 μM) in aqueous solution at pH = 12 and in DMSO; fluorescence excitation spectrum of **DiCPP-opp** (λ_{em} = 675 nm, pH = 12); and (B) fluorescence emission spectra of **DiCPP-opp** in aqueous solution at pH = 12 obtained at different excitation wavelengths: 416 nm (black) and 446 nm (grey).

The formation of a new fluorescent aggregate species at pH 12 can also be followed by steady-state fluorescence emission and some alterations dependent on the λ_{exc} are observed (Fig. 1B): at 446 nm excitation both emission bands suffer a ~15 nm red shift and are far less intense than those obtained at 416 nm excitation. This confirms that the fluorescence quantum yield of aggregated species is lower than that of monomers. Some important alterations dependent on the λ_{exc} can also be observed at pH 7: at 446 nm excitation, the two emission bands suffer a 9 nm red shift and in the same way far less intense bands than those obtained at 416 nm are observed. These aspects are in accordance with the absorption data obtained for **DiCPP-opp** with increasing pH values, reinforcing that the formation of the new aggregate species is favoured at higher pH values. The aggregate band with peaks at 446 nm and 365 nm increase with the porphyrin concentration suggesting the coexistence of two orientations in the aggregate (See Supporting Information, Fig. S1†).

There is a clear dependence on the nature of positively charged inorganic counterions in the aggregation features of this porphyrin as illustrated on Fig. 2 upon addition of LiOH, KOH and CsOH to an aqueous solution of **DiCPP-opp** at pH 12. In the presence of K^+ and Cs^+, no aggregation was observed (λ_{max} = 416 and 414 nm, respectively), but a J-aggregate band at 440 nm appears in the aqueous solution of LiOH. We believe that this effect has not been previously reported.

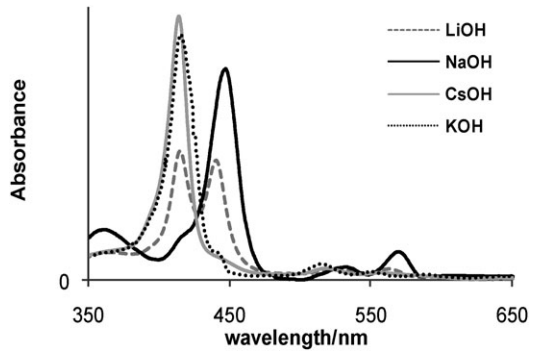

Fig. 2 Counterion effect on UV-Vis spectra of **DiCPP-opp** (5 μM) in aqueous solution at pH 12. [X^+] = 0.01 M and X = Na, Li, K, or Cs.

At pH 0.8, the absorption spectrum is different from the previous one. It exhibits two broader bands clearly overlapped, one at 436 and the other at 496 nm (See Supporting Information, Fig. S2†). The co-existence of non-specific aggregates leads to broader bands over the entire spectrum.

DiCPP-adj. The absorption spectra of **DiCPP-adj**, with the two carboxyphenyl groups in adjacent positions, outline the aggregation profile of this porphyrin at acidic conditions. A very clear aggregation pattern in HNO_3 aqueous solutions at pH = 0.8 is observed unequivocally with this porphyrin: sharp well defined red-shifted absorption bands both in the Soret

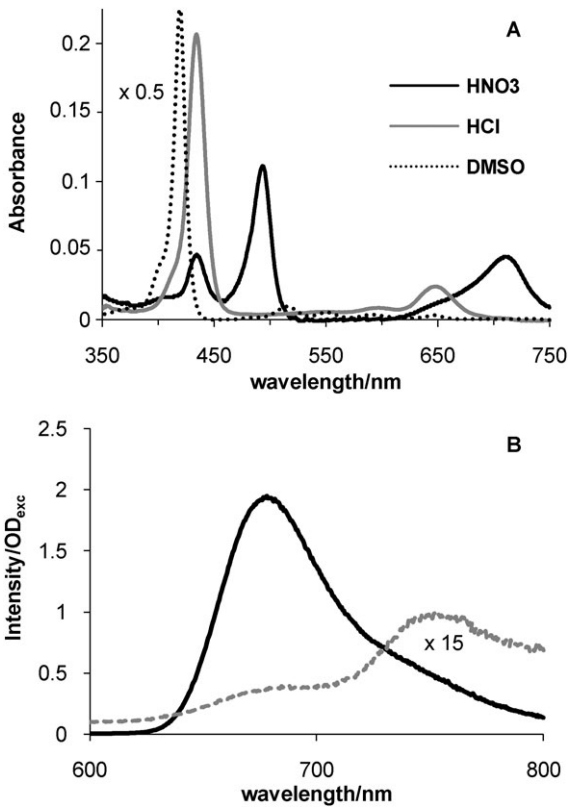

Fig. 3 (A) UV-Vis spectra of **DiCPP-adj** (5 μM) in aqueous solution at pH = 0.8 and in DMSO; and (B) fluorescence emission spectra of **DiCPP-adj** in aqueous HNO_3 (pH = 0.8) obtained at different excitation wavelengths: 436 nm (black) and 496 nm (grey).

Published on 26 August 2010 on http://pubs.rsc.org | doi:10.1039/C0NJ00201A
Downloaded by University of Belgrade on 02 January 2013

(494 nm) and in the Q-band region (713 nm) are characteristic of a J-aggregate based on the di-acid porphyrin (Fig. 3A). These features are enhanced both by an increase in the solution's ionic strength, as well as by a concentration increase (see Supporting Information, Fig. S3†). Moreover, a clear dependence on the counter-ion nature is observed, since no aggregation is detected at this pH with the addition of Cl^- or SO_4^{-2} (Fig. 3A). Such aggregation dependence had already been reported for *meso*-tetrakis(4-carboxyphenyl)porphyrin, TCPP, in aqueous acidic solutions of HNO_3 at pH lower than 1; but in this case, the presence of a PVA stabilizer was required.[7]

In agreement with the absorption data, the fluorescence spectra of **DiCPP-adj**, suggest also the formation of a J-aggregate based on the dicationic porphyrin at pH 0.8: the main band centered at 678 nm corresponds to the monomer fluorescence whereas a new less intense band is obtained in the red upon excitation in the aggregate absorption band (Fig. 3B). Although the excitation spectra depend on the emission wavelength, the contribution from the monomer clearly dominates that of the aggregate, pointing to a very low fluorescence quantum yield of the J-aggregate, as was reported for TSPP J-aggregate ($\phi_f \sim 10^{-3}$).[13]

By contrast to the strong aggregation found at pH = 0.8, under alkaline conditions (pH = 7, 10, 12) and comparatively to **DiCPP-opp** this porphyrin presents less tendency to self-aggregate as denoted by the absence of new absorption bands. Instead a broad Soret band is observed with a maximum at a similar wavelength to that obtained in DMSO (Table 1). In the fluorescence emission there is a 2 nm red shift which can be detected in the pH range of 7 to 12 (see Supporting Information, Fig. S4†), and blue- and red-shoulders in the Soret band visible in fluorescence excitation spectra (data not shown).

The aggregate's stability was periodically checked by means of absorption and fluorescence spectroscopy (see Supporting Information, Fig. S5). At pH 12, these spectra remain the same even after weeks of storage denoting their high stability. Still, after a few days, it's possible to denote the formation of a green precipitate in solutions prepared at pH 0.8. Curiously, the precipitates of dicationic porphyrins disappear simply by mixing the solution and the opalescence characteristic of the porphyrin aggregate reappears. In this case, the absorption and fluorescence spectra are also restored.

For comparison purposes, regarding the effect of the number of *meso*-carboxyphenyl substituents in the aggregation behavior, 5-(4-carboxyphenyl)-10,15,20-tri-phenylporphyrin (MCPP) was also checked under the same experimental conditions. Interestingly, we have found that MCPP, with only one *meso*-carboxyphenyl group, shows similar aggregation patterns to both disubstituted porphyrins **DiCPP-opp** and **DiCPP-adj** (data not shown): at pH = 12, and similarly to **DiCPP-opp**, a new J-band at 448 nm can be observed; at pH 0.8, and similarly to **DiCPP-adj**, a putative aggregate can be responsible for the red shifted bands at 494 and 714 nm. Curiously, at both pH conditions, this porphyrin shows less tendency to form aggregates than **DiCPP-opp** and **DiCPP-adj**, as denoted by the presence of intense absorption bands typical of the monomeric species.

Fluorescence lifetimes of substituted porphyrins in solution

Fluorescence decays were obtained upon laser excitation at 405 nm for all the porphyrins studied in aqueous solution (pH = 0.8 and 12) and compared to the corresponding ones in DMSO. In organic solvents, fluorescence decays are dominated by a long component similar to what had been previously reported for other *meso*-phenyl porphyrins (see Table 2).[9,14,15] Nevertheless, there is still a ~10% contribution from a short lifetime which is similar in both cases of **DiCPP-opp** and **DiCPP-adj**. For instance, in the case of the free-base form of TSPP, a second lifetime around 7 ns was obtained in DMSO, the value being shorter in a protic solvent like methanol (~5.6 ns). Since molecular aggregation can drastically decrease fluorescence decay times, the shorter lived components may be assigned to the fluorescent non-specific aggregate species. Therefore, the existence of aggregates is also favoured in this type of solvent, although the possibility of traces of water inducing aggregation cannot be discarded. The intermediate lifetime values are usually associated to dimers whereas the very short lifetimes are assigned to oligomeric species. In aqueous solution at pH 12, the best fit is only achieved using a 3-exponential approach. Although the fluorescence decay has a long component, it is clearly dominated by short lived components. By comparison with the long-lived component obtained for these porphyrins in DMSO, we can assign this contribution to the existence of monomers at high pH. This assumption agrees well with the UV-Vis and emission spectra. Moreover, while there is also a shorter component with a lifetime similar to that obtained in DMSO for both porphyrins an intermediate component was also detected implying the co-existence of dimers and higher order aggregates. According to the overall data, in aqueous solution at basic pH, the aggregation is possible in **DiCPP-opp**. Under the same conditions of excitation/emission used for DMSO and alkaline porphyrin solutions, at pH = 0.8, two lifetimes were obtained, one of 3.54 ns and a short-lived component of 360 ps detected with less than 30% contribution. The direct excitation on the J-aggregate band (483 nm laser) confirms the same two components but with 97% contribution from the short component. The fluorescence decays at pH 0.8 could also be obtained using monochromatic excitation and emission light at each peak (λ_{exc} = 434 nm and λ_{em} = 680 nm), from which a single fluorescence lifetime of 3.45 ns could be retrieved. This value is only slightly shorter than the one

Table 2 Fluorescence lifetimes of substituted *meso*-carboxyphenyl porphyrins obtained in aqueous solution at different pH and in DMSO

Porphyrin	pH	A_1 (%)	τ_1/ns	A_2 (%)	τ_2/ns	A_3 (%)	τ_3/ns
DiCPP-opp	0.8	79.5	3.50	—	—	20.5	0.495
	12	12.0	9.65	21.9	2.28	66.1	0.644
	12[a]	14.9	9.65	23.3	2.28	61.8	0.644
	12[b]	63.1	9.65	26.9	2.28	10.0	0.644
	DMSO	89.0	11.20	—	—	11.0	0.650
DiCPP-adj	0.8	70.4	3.54	—	—	29.6	0.360
	0.8[c]	2.6	3.54	—	—	97.4	0.360
	12	20.9	9.59	25.3	3.32	53.8	0.669
	DMSO	92.3	11.14	—	—	7.67	0.750

[a] Li^+. [b] Cs^+. [c] Exc = 483 nm.

 This journal is © The Royal Society of Chemistry and the Centre National de la Recherche Scientifique 2010

Published on 26 August 2010 on http://pubs.rsc.org | doi:10.1039/C0NJ00201A
Downloaded by University of Belgrade on 02 January 2013

reported for the di-acid form of TSPP (~3.8 ns) at pH = 2,[9,13,15] thus, corresponding to porphyrin monomers with protonated inner nitrogen atoms. Based on this data, the order of aggregation tendency at pH = 0.8 using HNO_3 is **DiCPP-adj** > **DiCPP-opp**.

Aggregation studies by resonance light scattering

Pasternack and co-workers reported that RLS can be used with equal feasibility as any other conventional techniques like steady-state or dynamic light scattering (DLS) for determining the size, shape and geometry of chromophore aggregates of porphyrins and chlorophylls.[16] Like absorption and fluorescence steady-state spectra, the RLS measurements give also important information supporting the postulated tendency of **DiCPP-opp** and **DiCPP-adj** to produce pH induced aggregates.

Fig. 4A and B display the RLS profile of **DiCPP-opp** and **DiCPP-adj** obtained at the two significant pH experimental conditions. Specific large resonance peaks are observed for **DiCPP-opp** at pH = 12 and for derivative **DiCPP-adj** at pH = 0.8. Since the spectra show enough RLS signals to overcome the absorption effects, a large number of interacting molecules must be involved in the aggregate structural arrangement. Note that less intense RLS signals are also observed in the Q-band region for **DiCPP-opp**.

It is important to point out that the intensity of RLS signals is higher for **DiCPP-opp** than for MCPP at pH 12 (data not shown). Since the intensity signal of the RLS peak depends on the size of the aggregate formed, we are tentatively assuming that the introduction of the second carboxyphenyl substituent can improve the tendency for aggregation. On the other hand, the RLS signal observed for the di-substituted **DiCPP-adj** at pH = 0.8, is sharper than that of **DiCPP-opp**, reflecting that in an acidic medium the former has a higher propensity for aggregation than the latter and/or there is a higher excitonic coupling in this aggregate.

Aggregation studies by circular dichroism

Circular dichroism spectroscopy is also considered a powerful tool for the detection of reasonably organized aggregates.[17]

The compounds studied when present in the monomeric form are achiral and it is expected that they are devoid of any CD signal. However at the key pHs a bisignate Soret CD signal can be observed for **DiCPP-adj** and **DiCPP-opp** in the Soret region, which is clear evidence of electronic interaction between the monomeric porphyrins (Fig. 5). In a disordered environment, such as a disordered aggregate, the elements do not show preferential interaction with either right- or left-handed circularly polarized light. However, when a supramolecular architecture is formed, the spatial arrangement may have chirality, even when the individual chromophores are optically silent, and a Cotton effect can be observed. Moreover, the fact that the CD signal is accompanied by the RLS signal further points to an intrinsically chiral exciton involving mutual porphyrin interactions.

The Cotton effect of **DiCPP-adj** at pH 0.8 is much more pronounced than the one obtained for **DiCPP-opp** at the same pH.

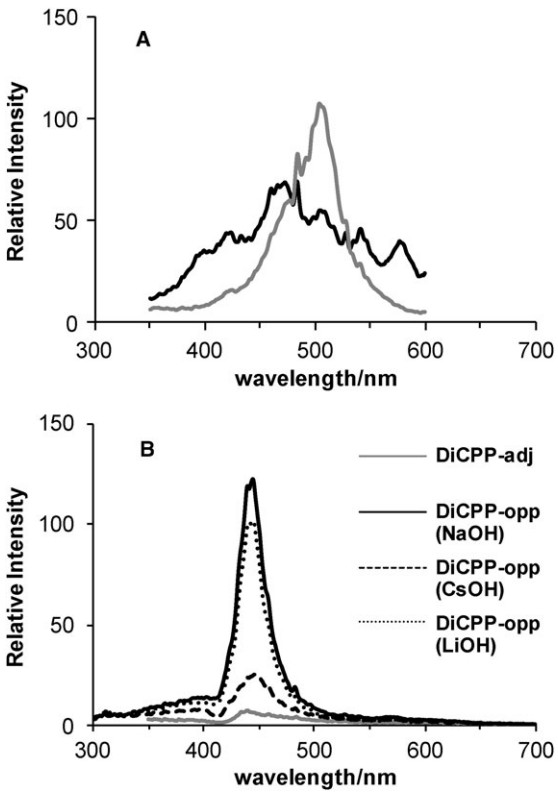

Fig. 4 RLS spectra of **DiCPP-opp** (black) and **DiCPP-adj** (grey) in aqueous solution at (A) pH = 0.8 with HNO_3 and (B) pH = 12 with different counterions.

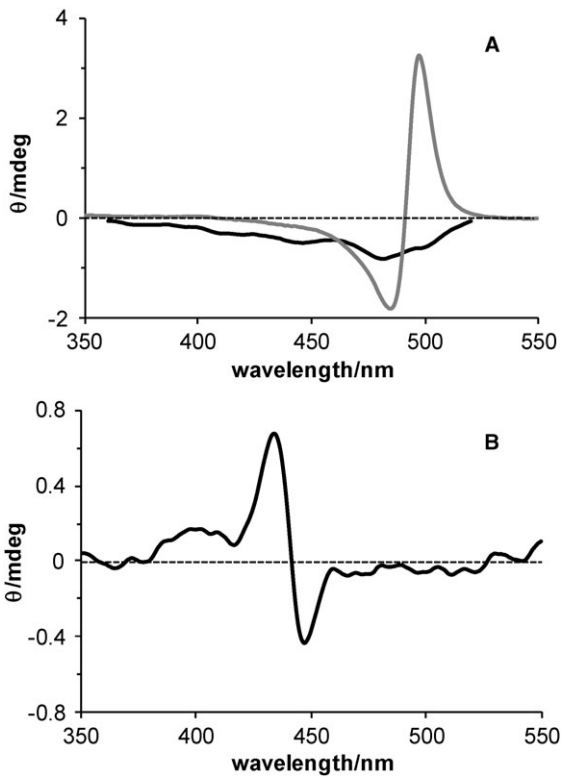

Fig. 5 CD spectra of di-substituted porphyrins obtained in aqueous solution at (A) pH = 0.8 (HNO_3) and (B) pH = 12: **DiCPP-opp** (black) and **DiCPP-adj** (grey).

Published on 26 August 2010 on http://pubs.rsc.org | doi:10.1039/C0NJ00201A
Downloaded by University of Belgrade on 02 January 2013

Fluorescence lifetime imaging microscopy (FLIM)

We have used the FLIM technique to elucidate the sizes and shapes of the carboxylic porphyrin aggregates. To this end, the fluorescence intensity of an image is followed both in time and space. The analysis with an exponential model allows us to retrieve the decay times which are then used to map the corresponding images and thus to provide the fluorescence lifetime imaging (optical resolution is diffraction-limited $\sim\lambda_{exc}/2$). The 638 nm excitation wavelength was chosen in order to minimize scattered light contamination without affecting the fluorescence decays of the porphyrins under study.

FLIM images of **DiCPP-opp** (pH = 12) and of **DiCPP-adj** (pH = 0.8) samples deposited on a glass coverslip, are depicted in Fig. 6A and B, respectively. Both images exhibit the presence of circular structures (including rings) with average diameters of 1–4 μm. Although the accuracy of size determination from these images is conditioned by the non-homogeneous film thickness, the estimated sizes are in reasonable agreement with DLS[18] measurements in solution thus pointing to micrometric structures of porphyrin aggregates.

The FLIM for the **DiCPP-opp** sample shows a tri-exponential fluorescence decay per pixel. The parameters adjusted from the decays show a long decay time component of approximately 10 ns, which is in good agreement with that obtained in solution and may thus be assigned to **DiCPP-opp** dispersed as monomer. By contrast, the short components of approximately 2.4 ns and 0.65 ns may be due to aggregated species (or from dynamic processes that involve energy transfer between monomers) also consistent with data obtained in solution.

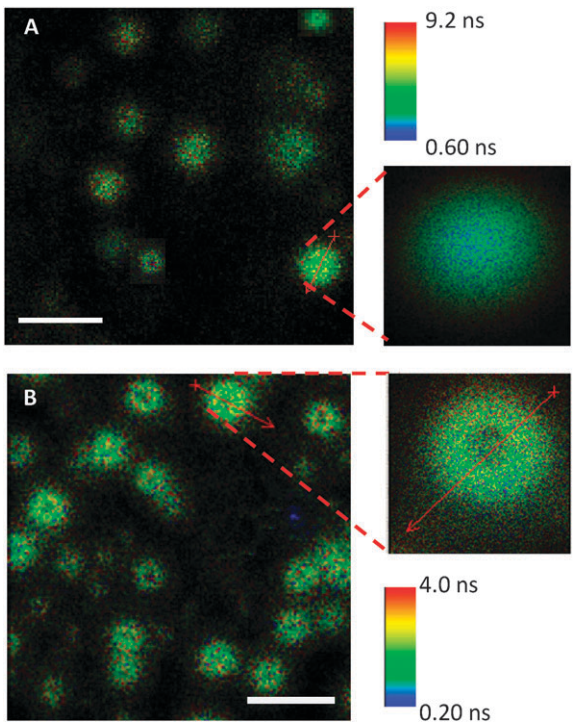

Fig. 6 Representative FLIM images of (A) **DiCPP-opp** at pH = 12 (NaOH) and of (B) **DiCPP-adj** at pH = 0.8 (HNO_3) deposited on a glass coverslip (white bar equivalent to 5 μm). A′, B′: Zooms of the marked region (emphasizing the most common structures imaged).

In the case of **DiCPP-adj** (Fig. 6B), the existence of dispersed **DiCPP-adj** monomers can also be inferred from a longer component (approximately 4 ns) resembling the result obtained in solution. The FLIM image also points out the predominance of short components of roughly 1.5 ns and 0.35 ns, the latter being in close agreement with the value obtained in solution.

Discussion

The results show that different experimental pH conditions are necessary to induce the growth of aggregated species of *meso*-carboxyphenylporphyrins **DiCPP-opp** and **DiCPP-adj** in water solutions containing a small percentage of a co-solvent (<5%) and in the absence of a stabilizer. Changes in the aggregation patterns observed are likely due to the different structural features of porphyrins under analysis.

pH = 0.8

The UV/vis spectra of porphyrins presented in this study in aqueous solution gave evidence of the presence of different species depending on the pH. There was a clear dependence on the acidifying agent, with HNO_3 inducing the porphyrins' self-aggregation by contrast to H_2SO_4 and HCl. At pH 0.8, the porphyrins assume a dicationic form, so at low pH values negative ions are needed in the surroundings to compensate the charge. It is possible that the formation and stability of the J-aggregate with the NO_3^- ions may be due to an extra co-planar binding that it is not possible with Cl^- or SO_4^{-2} anions. So, we are tentatively assuming that the nitrate ion can effectively participate in the aggregates's arrangement, either by electrostatic interactions or by π–π interactions between the nitrate and the macrocycle. The counterion can act as a bridge between the inner protons of neighbour porphyrins. A similar counterion dependent aggregation behaviour had been reported before with TCPP.[7] The formation of counterion-dependent assemblies are also invoked in the aggregate behaviour of 5,10,15,20-tetrakis(3,5-dimethoxyphenyl)-21*H*,23*H*-porphine (H_2TPPDOMe) in acidic media.[19] The enhancement of the J-band with increasing ionic strength suggests that the acidic medium provides not only the protons needed for the total protonation of the inner nitrogen atoms, but also a high concentration of counter-anions.

Comparative to TCPP, **DiCPP-adj** presents spectroscopic features more similar to those of TSPP and leads to stable J-aggregates in acidic water. In the case of TSPP its zwitterionic nature leads to Coulombic interactions between the positively charged macrocycle of one unit and the negatively charged sulfonate peripheral groups of the next. Porphyrins with carboxylic peripheral groups have these groups uncharged at this low pH; then those interactions are absent. Therefore, the counterion (unimportant in TSPP) performs a crucial role in this case. Since there are carboxylic groups, it is possible that these molecules interact with each other by hydrogen bonding. Alternatively, there may be hydrophobic interactions between the phenyl groups (Scheme 2A). **DiCPP-adj** J-aggregates may arrange helicoidally. Therefore, one is tempted to envisage a competition between inter-molecular H-bonding of porphyrin units and those involving

 This journal is © The Royal Society of Chemistry and the Centre National de la Recherche Scientifique 2010

Published on 26 August 2010 on http://pubs.rsc.org | doi:10.1039/C0NJ00201A
Downloaded by University of Belgrade on 02 January 2013

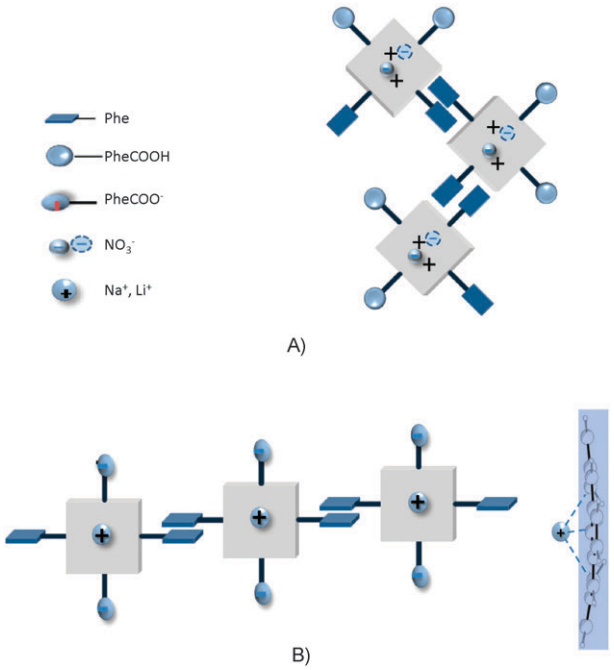

Scheme 2 Possible structural models for the aggregate structure: hydrogen bonding and the counterion are the main interactions that will induce the growth of porphyrinic arrays in (A) layer-by-layer directions in **DiCPP-adj**, pH = 0.8 or end-to-end in (B) **DiCPP-opp**, pH = 12, front and side views.

water molecules. The role of the counterion in the induction of porphyrin J-aggregates was also pointed out for a series of *meso*-phenyl porphyrins at the CH_2Cl_2–aqueous H_2SO_4 interface.[20] A study by Pasternack *et al.*,[21] showed that unlike TSPP, the trisulfonated porphyrin ($TSPP_3$) J-aggregation in the pH range 1–3 depended on the electrolyte nature. Its importance can not only be seen by the electrostatic interactions provided but also through its effect on the network structure of water molecules. The empirical Hoffmeister series was developed from ranking various ions toward their ability to precipitate a mixture of hen egg white proteins.[22] The hypothesis of relating here the counter-ion effects seems pertinent. Structure-breaking anions disrupt water-structure thus enhancing the protein solubility. Nitrate ions are considered more structure-breaking whereas sulfate and citrate are considered structure-making and chloride ions lie in the middle of the series.

It is worth noting that the J-aggregates formed in the diprotonated system contributed more dramatically to spectral changes than the ones obtained for the J-aggregates of free-base porphyrins which points to stronger intermolecular interactions on the charged ring. Upon acidification, a more planar conformation of the porphyrin is achieved which is known to contribute to an enhanced ''communication'' between porphyrin units.[23]

Intermediate pHs

At a pH range between 2 and 5, the absorbance decreases giving evidence of a broad Soret band with a shoulder at 405 nm and a considerable loss in fluorescence intensity. No isosbestic points were detected for any of the porphyrins studied which is a clear indication of co-existence of several species at the pH range explored. An etio pattern of the Q-bands points to an apparent change in the protonation of the nitrogen atoms which lowers the symmetry from the D_{4h} of the di-acid monomer to D_{2h} as in the free-base form. These perturbations in the Q-bands can be indicative of a rather low pK_a comparative to those reported for other *meso*-substituted porphyrins[24] or can be due to aggregation and interpreted in terms of the existence of specific interactions between peripheral groups and the inner core, *e.g.*: H-bonds. Interestingly, extended supramolecular structures, such as fibers, micellar rods and vesicular tubules, stabilized through hydrogen bonding between partially neutralized carboxylic acid side chains were reported for (derivatized) protoporphyrin IX at intermediate pHs.[25]

pH ≥ 7

Similar to the acidic pH range, the number and position of the carboxylic acid group determines the self-association process of the porphyrins presented in this study. Spectral differences as well as fluorescence lifetimes also point out the importance of the ionization state of the carboxylate groups. The metal ions, Na^+ and Li^+ with a small ionic radii can interact with the nitrogen atoms of the porphyrin core as suggested in the literature.[26] A distortion of the macrocycle induces a rotation of the phenyl rings. Herein, the stacking of the unsubstituted phenyl groups of neighbour porphyrin rings may occur whereas the phenylcarboxylate groups are oriented perpendicular to the macrocycle chain avoiding electrostatic repulsions. The extended arrays of J-aggregates in **DiCPP-opp** may thus be understood in terms of Scheme 2B. A similar arrangement is not possible for **DiCPP-adj** where only dimers may be found.

5,10,15,20-Tetrakis[4-(*N*-methyl)pyridinium]-porphyrin, TMPyP, a tetracationic porphyrin, exists as a monomer in aqueous solution regardless of the presence of salts,[27] whereas the cationic derivative, 5,15-diphenyl-10,20-bis[4-(*N*-methyl) pyridinium] porphyrin, DiMPyP-opp, readily forms large aggregates.[28] Curiously, J-aggregates were detected for $TSPP_2$-opp and $TSPP_1$[29] with the Soret peak close to the ones we have obtained with the carboxylic derivatives; but not for $TSPP_2$-adj, nor for **DiCPP-adj**.

The results described in this article may be potentially interesting for the design of photoactive materials, namely for applications in nanodevices and in light harvesting complexes. Moreover, the possibility to tune the morphology of these molecular assemblies (changing pH, anion/cation) enable us to envisage their possible role as sensors.

Conclusions

Meso-dicarboxyphenyl porphyrins **DiCPP-opp** and **DiCPP-adj** form spontaneously pH induced aggregates in aqueous solutions. At pH = 0.8, the adjacent carboxylic groups in **DiCPP-adj** are not charged and the counterion (NO_3^-) plays a crucial role in the establishment of highly ordered J-aggregates mediated either by the nitrate anion or by hydrogen bonding. Conversely, at pH = 12, both the effects of the metal

Published on 26 August 2010 on http://pubs.rsc.org | doi:10.1039/C0NJ00201A
Downloaded by University of Belgrade on 02 January 2013

counterion as well as the stacking of opposite phenyl groups in **DiCPP-opp** favour aggregation. The aggregates were detected by electronic absorption and emission, fluorescence lifetimes, resonance, dynamic light scattering, and circular dichroism. The fluorescence lifetime imaging technique, FLIM, shows ring aggregates of **DiCPP-adj** at pH = 0.8 which are likely associated to a helicoidal structure. At pH = 12, **DiCPP-opp** arrange end-to-end resulting in circular type aggregates detected by the same spectroscopic technique. The type of molecular architectures and the extent of aggregation are related to the relative positions of the 4-carboxyphenyl units attached to the porphyrin core.

Experimental section

Materials

Several buffer solutions of citrate-phosphate pH 2–7 were prepared in the range of pH 2–7 using bidistilled water, according to standard procedures. For pH = 0.8 and 12, aqueous solutions of HNO_3 or NaOH were used, unless mentioned otherwise. The benzaldehydes used in the synthesis of porphyrins (see Supporting information†) were purchased from Sigma-Aldrich (Madrid) and used as received. Pyrrole and all the solvents were used as received or distilled and dried using standard procedures.

Sample preparation

Stock solutions (0.25 mM) of **DiCPP-opp** and **DiCPP-adj** porphyrins were prepared in spectroscopic dimethyl sulfoxide. Each stock solution was stored in the dark and used within a month of preparation. The aggregates were obtained at the required pH by diluting a small volume of the porphyrinic stock solution (100 μl), keeping the final concentration of porphyrin at 5 μM. Then the resulting mixture was kept at 40 °C for 1 h.

Methods

Absorption spectra were scanned from 350 to 800 nm in a Jasco V-560 UV-Vis absorption spectrophotometer. RLS spectra were carried out in a Perkin-Elmer LS-50B spectrofluorimeter, by synchronous excitation and emission scanning in the right angle geometry and corrected by subtracting the correspondent blank sample. The electronic extinction spectra (absorption + scattering) were scanned from 350 to 800 nm in a Jasco V-560 UV-Vis spectrophotometer and corrected for the resonant scattering components occurring at the red-edge of the J-aggregate band.[30] This correction was made withdrawing the scattering contribution accounted for in RLS spectra obtained by synchronous excitation and emission scanning in the right angle geometry. A linear fitting of the extinction *vs*. RLS intensity in the region where the extinction light is solely due to resonant light scattering (*i.e.*: 485–515 nm, pH = 12; 510–590 nm, pH = 0.8), allows us to scale the RLS spectra which can then be subtracted from the extinction one to obtain the absorption contribution. The main differences detected between extinction and absorption spectra are intensity and narrowing of the J-band. Fluorescence steady-state measurements were carried out with a Fluorolog Tau-3 spectrofluorimeter. Corrected spectra were obtained using the correction file provided with the instrument. All the spectra were recorded at room temperature using a 1 cm path length quartz cuvette.

Fluorescence lifetimes using monochromated excitation (λ_{exc} = 430 nm) and emission (λ_{emi} = 675 nm) were retrieved using SPEX® Tau 3 (HORIBA Jobin Yvon) working in the frequency domain. In this case, the samples are excited by a modulated light source (Xenon lamp) at variable frequency (1 to 300 MHz). The sample response, collected by a conventional PMT, has a similar waveform but it is modulated and phase-shifted from the excitation curve. Phase-angle shift and demodulation ratio measured as a function of modulation frequency provide the way to calculate the sample lifetime. Fluorescence lifetimes were also obtained with a time-correlated single-photon counting (TC-SPC) technique using commercial equipment Microtime 200 from Picoquant GmbH. Excitation was achieved using a pulsed laser diode head at 405 nm (or at 483 nm), with varied repetition rate (10, 20 or 40 MHz). A band-pass filter with transmission in the range 600–800 nm was used to eliminate backscattered light in the photomultiplier tube from Picoquant (model PMA-182). Data analysis was performed by a deconvolution method using a non-linear least-squares fitting program, based on the Marquardt algorithm. The goodness of the fit was evaluated by the usual statistical criteria and by visual inspection of the weighted residual distribution and the autocorrelation function. FLIM was performed in the same setup and a more detailed description may be found elsewhere.[31] Briefly, the 638 nm excitation light from a pulsed diode laser was focused by an oil immersion objective ×100 with 1.3 NA, into the sample. Fluorescence was collected by the same microscope objective, passed through the dichroic mirror and appropriate band-pass filter (695AF55 Omega optical) and focused through a pinhole (50 μm), to reject out-of-focus light, onto a single-photon counting avalanche photodiode SPAD (Perkin-Elmer) whose signal was processed by TimeHarp 200 TC-SPC PC-board (PicoQuant) working in the special Time-Tagged Time-Resolved Mode, which stores all relevant information for every detected photon. CD spectra were obtained in a Jasco J-720 spectropolarimeter, using a 1 cm path length quartz cuvette. Five scans were performed for each 5 μM porphyrin solution when absorption and fluorescence emission typical bands of aggregate species were observed. The average spectrum was corrected by subtracting the corresponding blank sample. The temperature was stabilized at 24.0 ± 0.5 °C.

Acknowledgements

Thanks are due to Fundação para a Ciência e a Tecnologia (FCT, Portugal) and POCI 2010 (FEDER) for funding the Aveiro Organic Chemistry Research Unit. V. V. Serra also thanks FCT for her PhD grant (SFRH/BD/28122/2006). S. M. B. Costa and S. M. Andrade acknowledge the financial support from CQE/FCT, projects POCI/QUI/57387/2004, PTDC/QUI/64112/2006 and 3° Quadro Comunitário de Apoio (FEDER) and FCT/Re-equipment project 115/Qui/2004.

 This journal is © The Royal Society of Chemistry and the Centre National de la Recherche Scientifique 2010

View Article Online

Published on 26 August 2010 on http://pubs.rsc.org | doi:10.1039/C0NJ00201A
Downloaded by University of Belgrade on 02 January 2013

Notes and references

1 *The Porphyrin Handbook*, ed. K. M. Kadish, K. M. Smith and R. Guillard, Academic Press, San Diego, 2000, vol. 6.
2 X. Hu and K. Schulten, *Phys. Today*, 1997, **50**, 28–34.
3 W. I. White, in *The Porphyrins*, ed. D. Dolphin, Academic Press, New York, 1978, vol. 5, ch. 7.
4 A. Satake and Y. Kobuke, *Tetrahedron*, 2005, **61**, 13–41; K. Araki and H. E. Toma, *Química Nova*, 2002, **25**, 962–975.
5 E. Collini, C. Ferrante and R. Bozio, *J. Phys. Chem. B*, 2005, **109**, 2–5; N. Micali, F. Mallamace, A. Romeo, R. Purrello and L. M. Scolaro, *J. Phys. Chem. B*, 2000, **104**, 5897–5904; S. M. Andrade and S. M. B. Costa, *J. Fluoresc.*, 2002, **12**, 77–82; S. M. Andrade and S. M. B. Costa, *Chem.–Eur. J.*, 2006, **12**, 1046–1057; Z. El-Hachemi, G. Mancini, J. M. Ribó and A. Sorrenti, *New J. Chem.*, 2010, **34**, 260–266.
6 X. Li, D. Li, W. Zeng, G. Zou and Z. Chen, *J. Phys. Chem. B*, 2007, **111**, 1502–1506.
7 M. Y. Choi, J. A. Pollard, M. A. Webb and J. L. McHale, *J. Am. Chem. Soc.*, 2003, **125**, 810–820; S. C. Doan, S. Shanmugham, E. D. Aston and J. L. McHale, *J. Am. Chem. Soc.*, 2005, **127**, 5885–5892.
8 D. L. Akins, H.-R. Zhu and C. Guo, *J. Phys. Chem.*, 1996, **100**, 5420–5425; X. Gong, T. Milic, C. Xu, J. D. Batteas and C. M. Drain, *J. Am. Chem. Soc.*, 2002, **124**, 14290–14291.
9 N. C. Maiti, S. Mazumdar and N. Periasamy, *J. Phys. Chem. B*, 1998, **102**, 1528–1538.
10 M. A. Castriciano, A. Romeo, N. Angelini, N. Micali, A. Longo, A. Mazzaglia and L. M. Scolaro, *Macromolecules*, 2006, **39**, 5489–5496.
11 M. Kasha, *Radiat. Res.*, 1963, **20**, 55–71.
12 M. Gouterman, in *The Porphyrins*, ed. D. Dolphin, Academic Press, New York, 1978, vol. 3, ch. 1.
13 A. Miura, Y. Shibata, H. Chosrowjan, N. Mataga and N. Tamai, *J. Photochem. Photobiol., A*, 2006, **178**, 192–200.
14 S. M. Andrade, R. Teixeira, S. M. B. Costa and A. J. F. N. Sobral, *Biophys. Chem.*, 2008, **133**, 1–10.
15 S. M. Andrade and S. M. B. Costa, *Biophys. J.*, 2002, **82**, 1607–1619.
16 J. Parkash, J. H. Robblee, J. Agnew, E. Gibbs, P. Collings, R. F. Pasternack and J. C. de Paula, *Biophys. J.*, 1998, **74**, 2089–2099; P. J. Collings, E. J. Gibbs, T. E. Starr, O. Vafek, C. Yee, L. A. Pomerance and R. F. Pasternack, *J. Phys. Chem. B*, 1999, **103**, 8474–8481.
17 O. Ohno, Y. Kaizu and H. Kobayashi, *J. Chem. Phys.*, 1993, **99**, 4128–4139; X. Huang, K. Nakanishi and N. Berova, *Chirality*, 2000, **12**, 237–255; R. Rubires, J.-A. Farrera and J. M. Ribó, *Chem.–Eur. J.*, 2001, **7**, 436–446; Z. El-Hachemi, O. Arteaga, A. Canillas, J. Crusats, C. Escudero, R. Kuroda, T. Harada, M. Rosa and J. M. Ribó, *Chem.–Eur. J.*, 2008, **14**, 6438–6443.
18 Note: DLS experiments gave evidence for the existence of very large J-aggregates for both DiCPP-adj and DiCPP-opp at pH 0.8 and pH 12, respectively. Assuming a spherical model, for DiCPP-adj the size distributions of the particles are broad with mean diameters near to the upper limit of detection (4 to 6 μm). For DiCPP-opp, two distinct and narrow size distributions were obtained with mean diameters of 5 μm (major contribution) and 1.2 μm.
19 Y. Zhang, P. Chen, Y. Ma, S. He and M. Liu, *ACS Appl. Mater. Interfaces*, 2009, **1**, 2036–2043.
20 S. Okada and H. Segawa, *J. Am. Chem. Soc.*, 2003, **125**, 2792–2796.
21 R. F. Pasternack, P. R. Huber, P. Boyd, G. Engasser, L. Francesconi, E. Gibbs, P. Fasella, G. Cerio Venturo and L. C. Hinds, *J. Am. Chem. Soc.*, 1972, **94**, 4511–4517.
22 F. Hofmeister, *Arch. Exp. Pathol. Pharmakol.*, 1888, **24**, 247–260.
23 J. A. Shelnutt, X.-Z. Song, J.-G. Ma, S.-L. Jia, W. Jentzen and C. J. Medforth, *Chem. Soc. Rev.*, 1998, **27**, 31–41.
24 K. Kano, K. Fukuda, H. Wakami, R. Nishiyabu and R. F. Pasternack, *J. Am. Chem. Soc.*, 2000, **122**, 7494–7502.
25 J. H. Fuhrhop, C. Demoulin, C. Boettcher, J. Koning and U. Siggel, *J. Am. Chem. Soc.*, 1992, **114**, 4159–4165; L. M. Scolaro, M. A. Castriciano, A. Romeo, S. Patanè, E. Cefalí and M. Allegrini, *J. Phys. Chem. B*, 2002, **106**, 2453–2459.
26 G. De Luca, A. Romeo, L. M. Scolaro, G. Ricciardi and A. Rosa, *Inorg. Chem.*, 2009, **48**, 8493–8508; J. J. A. van Kampen, T. M. Luider, P. J. A. Ruttink and P. C. Burgers, *J. Mass Spectrom.*, 2009, **44**, 1556–1564.
27 K. Kano, K. H. Minamizono, T. Kitae and S. Negi, *J. Phys. Chem. A*, 1997, **101**, 6118–6124.
28 R. F. Pasternack, C. Bustamante, P. J. Collings, A. Giannetto and E. J. Gibbs, *J. Am. Chem. Soc.*, 1993, **115**, 5393–5399.
29 R. Rubires, J. Crusats, Z. El-Hachemi, T. Jaramillo, M. López, E. Valls, J.-A. Farrera and J. M. Ribó, *New J. Chem.*, 1999, **23**, 189–198.
30 N. Micali, F. Mallamace, M. A. Castriciano, A. Romeo and L. M. Scolaro, *Anal. Chem.*, 2001, **73**, 4958–4963.
31 S. M. Andrade, S. M. B. Costa, J. W. Borst, A. van Hoek and A. J. W. Visser, *J. Fluoresc.*, 2008, **18**, 601–610.